



**INFLUENCE OF CNT, TiO₂ AND SiC NANOSTRUCTURE ADDITIONS ON
MICROSTRUCTURAL AND SUPERCONDUCTING PROPERTIES OF
YBa₂Cu₃O_{7-δ} SYNTHESIZED USING THERMAL TREATMENT**

By

BAROOD FATMA ALI ALFIRGANI

**Thesis Submitted to the School of Graduate Studies, Universiti Putra Malaysia, in
Fulfilment of the Requirements for the Degree of Doctor of Philosophy**

October 2023

FS 2023 13

All material contained within the thesis, including without limitation text, logos, icons, photographs and all other artwork, is copyright material of Universiti Putra Malaysia unless otherwise stated. Use may be made of any material contained within the thesis for non-commercial purposes from the copyright holder. Commercial use of material may only be made with the express, prior, written permission of Universiti Putra Malaysia.

Copyright © Universiti Putra Malaysia



Abstract of thesis presented to the Senate of Universiti Putra Malaysia in fulfilment of the requirement for the degree of Doctor of Philosophy

INFLUENCE OF CNT, TiO₂ AND SiC NANOSTRUCTURE ADDITIONS ON MICROSTRUCTURAL AND SUPERCONDUCTING PROPERTIES OF YBa₂Cu₃O_{7- δ} SYNTHESIZED USING THERMAL TREATMENT

By

BAROOD FATMA ALI ALFIRGANI

October 2023

Chair : Associate Professor Mohd Mustafa Awang Kechik, PhD
Faculty : Science

Yttrium Barium Copper Oxide YBa₂Cu₃O_{7- δ} (Y123) has emerged as one of the most promising high-temperature superconductors due to its potential applications in various fields. However, in high magnetic fields, Y123 applications are limited by weak links at grain boundaries, leading to low J_c . In this research, different weight percentages, $x = (0.0, 0.2, 0.4, 0.6, 0.8, \text{ and } 1.0 \text{ wt.}\%)$ of CNT (2 nm), TiO₂ (6 - 15 nm) and SiC (15 nm) nanostructures were added to Y123 bulk prepared using a thermal treatment method. The primary objective is to investigate how the incorporation of these nanostructures influences the structure and superconducting properties of Y123. The samples were characterised using various analytical techniques, including thermogravimetric analysis (TGA), X-ray diffraction (XRD), field emission scanning electron microscopy (FESEM) along with EDX, alternating current susceptibility (ACS), four-point probe technique (4PP) and electron-spin resonance (ESR). The XRD analysis revealed that the samples predominantly consisted of the Y123 phase, which exhibited an orthorhombic crystal structure. Additionally, the Y211 phase was detected in all additional samples as a minor phase. FESEM observations showed that the incorporation of CNT, TiO₂ and SiC nanostructures yielded more homogeneous specimens and improved inter-grain connectivity. EDX spectra performed for all Y123 samples showed the presence of Y, Ba, Cu and O elements with a precise match for the standard peak position for these elements. From ACS measurement, the presence of CNT enhanced onset critical temperature ($T_{c\text{-onset}}$) at $x = 0.4 \text{ wt.}\%$ CNT. Samples with the addition of TiO₂ and SiC showed a slight decrease in $T_{c\text{-onset}}$, while T_{c_j} greatly increased except for the higher contents of SiC. The temperature-dependent resistivity measurements, ρ - T confirmed the occurrence of superconductivity in all samples. However, samples at $x = 0.8$ and $1.0 \text{ wt.}\%$ SiC showed semiconducting like behaviour. $T_{c\text{-onset}}$ was observed at 95.6 K for a pure sample, and slightly decreased with the addition of nanostructures due to oxygen modification. The value of J_c as measured by current-voltage measurement was 2.08 A/cm² for the pure sample and increased to 8.1 A/cm² for the sample with $x = 0.4 \text{ wt.}\%$ CNT, indicating enhanced grain connectivity. The ESR spectra for all samples displayed a symmetrical signal behaviour. Based on the results obtained, it can be concluded that

the incorporation of CNT, TiO₂ and SiC nanostructures into Y123 superconductors offers a viable route to enhance the superconducting properties with the best result achieved at $x = 0.4$ wt.% CNT in term of $T_{c-onset}$ and J_c .



Abstrak tesis yang dikemukakan kepada Senat Universiti Putra Malaysia sebagai memenuhi keperluan untuk ijazah Doktor Falsafah

PENGARUH PENAMBAHAN NANOSTRUKTUR CNT, TiO₂ DAN SiC TERHADAP SIFAT MIKROSTRUKTUR DAN MENSUPERKONDUKSI YBa₂Cu₃O_{7-δ} YANG DISINTESIS MENGGUNAKAN RAWATAN TERMA

Oleh

BAROOD FATMA ALI ALFIRGANI

Oktober 2023

Pengerusi : Profesor Madya Mohd Mustafa Awang Kechik, PhD
Fakulti : Sains

Yttrium Barium Copper Oxide YBa₂Cu₃O_{7-δ} (Y123) telah muncul sebagai salah satu superkonduktor suhu tinggi yang paling menjanjikan kerana aplikasinya yang berpotensi dalam pelbagai bidang. Walau bagaimanapun, dalam medan magnet yang tinggi, aplikasi Y123 dihadkan oleh pautan lemah pada sempadan butiran, yang membawa kepada J_c yang rendah. Dalam penyelidikan ini, peratusan berat yang berbeza, $x = (0.0, 0.2, 0.4, 0.6, 0.8, \text{ dan } 1.0 \text{ wt.}\%)$ CNT (2 nm), TiO₂ (6 - 15 nm) dan SiC (15 nm) telah ditambah kepada Y123 pukal yang disediakan menggunakan kaedah rawatan terma. Objektif utama adalah untuk menyiasat bagaimana penggabungan struktur nano ini mempengaruhi struktur dan sifat mensuperkonduksi Y123. Sampel dicirikan menggunakan pelbagai teknik analisis, termasuk analisis termogravimetri (TGA), belauan sinar-X (XRD), mikroskop elektron pengimbasan pelepasan medan (FESEM) bersama-sama dengan EDX, kerentanan arus ulang-alik (ACS), teknik prob empat titik (4PP) dan resonans putaran elektron (ESR). Analisis XRD mendedahkan bahawa sampel kebanyakannya terdiri daripada fasa Y123, yang mempamerkan struktur kristal ortorombik. Selain itu, fasa Y211 dikesan dalam semua sampel tambahan sebagai fasa minor. Pemerhatian FESEM menunjukkan bahawa penggabungan struktur nano CNT, TiO₂ dan SiC menghasilkan lebih banyak spesimen homogen dan meningkatkan ketersambungan antara butiran. Spektrum EDX yang dilakukan untuk semua sampel Y123 menunjukkan kehadiran unsur Y, Ba, Cu dan O dengan padanan yang tepat bagi kedudukan puncak piawai untuk unsur-unsur ini. Daripada pengukuran ACS, kehadiran CNT telah meningkatkan suhu kritikal permulaan CNT ($T_{c\text{-onset}}$) pada $x = 0.4 \text{ wt.}\%$ CNT. Sampel dengan penambahan TiO₂ dan SiC menunjukkan sedikit penurunan dalam $T_{c\text{-onset}}$, manakala T_{c_j} meningkat dengan banyak kecuali bagi kandungan SiC yang lebih tinggi. Pengukuran kerintangan kebergantungan suhu, ρ - T mengesahkan berlakunya superkonduktiviti dalam semua sampel. Walau bagaimanapun, sampel pada $x = 0.8$ dan $1.0 \text{ wt.}\%$ SiC menunjukkan tingkah laku seperti semikonduktor. $T_{c\text{-onset}}$ diperhatikan pada 95.6 K untuk sampel tulen, dan sedikit berkurangan dengan penambahan struktur nano akibat pengubahsuaian oksigen. Nilai J_c seperti yang diukur dengan pengukuran voltan semasa ialah 2.08 A/cm^2 untuk sampel tulen dan meningkat kepada 8.1 A/cm^2 untuk

sampel dengan $x = 0.4$ wt.% CNT, menunjukkan peningkatan ketersambungan butiran. Spektrum ESR untuk semua sampel menunjukkan tingkah laku isyarat simetri. Berdasarkan keputusan yang diperoleh, dapat disimpulkan bahawa penggabungan struktur nano CNT, TiO_2 dan SiC ke dalam superkonduktor Y123 menawarkan laluan yang berdaya maju untuk meningkatkan sifat superkonduktor dengan hasil terbaik dicapai pada $x = 0.4$ wt.% CNT dalam istilah $T_{c\text{-onset}}$, dan J_c .



ACKNOWLEDGEMENTS

Alhamdulillahirabbil'alamin, all praises to Allah for the strengths and His blessing in completing this thesis. Special appreciation and sincere thanks go to my supervisor Assoc. Prof. Mohd Mustafa Bin Awang Kechik, for his supervision and constant support. His invaluable help of constructive comments and suggestions throughout the experimental and thesis works have contributed to the success of this research. My greatest gratitude and appreciation go to all my group members and staff in the superconductor lab, department of physics for sharing the literature and invaluable assistance. Thanks for the friendship and memories.

My deepest gratitude goes to my beloved parents; Mr. Ali Alfirgani and Mrs. Am Almeer Amar, my sisters and brothers for their endless love, prayers and encouragement.

My deepest gratitude and love go to my dear husband, Mr. Abdulsalam Mohamed for his sacrifices, tolerance, moral support, continuing love and prayers throughout this lengthy journey. Also, to my lovely kids.

This thesis was submitted to the Senate of Universiti Putra Malaysia and has been accepted as fulfilment of the requirement for the degree of degree of Doctor of Philosophy. The members of the Supervisory Committee were as follows:

Mohd Mustafa bin Awang Kechik, PhD

Associate Professor
Faculty of Science
Universiti Putra Malaysia
(Chairman)

Abdul Halim bin Shaari, PhD

Professor
Faculty of Science
Universiti Putra Malaysia
(Member)

Chen Soo Kien, PhD

Professor
Faculty of Science
Universiti Putra Malaysia
(Member)

ZALILAH MOHD SHARIFF, PhD

Professor and Dean
School of Graduate Studies
Universiti Putra Malaysia

Date: 14 March 2024

TABLE OF CONTENTS

		Page
	ABSTRACT	i
	ABSTRAK	iii
	ACKNOWLEDGEMENTS	v
	APPROVAL	vi
	DECLARATION	viii
	LIST OF TABLES	xiii
	LIST OF FIGURES	xv
	LIST OF ABBREVIATIONS	xxii
	CHAPTER	
1	INTRODUCTION	1
1.1	Superconducting Phenomenon: its Discovery and Evolution	1
1.2	High-Temperature Superconductivity (HTSC): A history	2
1.3	Applications of High- T_c Superconductors	3
1.4	Problem Statement	4
1.5	Research Objectives	5
1.6	Outline of the Thesis	5
2	FUNDAMENTAL THEORIES ON SUPERCONDUCTING PHENOMENA	6
2.1	Introduction	6
2.2	Origins of the Theory of Superconductivity	6
2.3	The BCS (Bardeen-Cooper-Schrieffer) Theory	7
2.4	Anisotropic Ginzburg-Landau Theory	8
2.5	Superconducting Gap	9
2.6	Principle Properties of the Superconducting State	10
2.6.1	Zero Electrical Resistivity	10
2.6.2	The Meissner-Ochsenfeld Effect	11
2.6.3	The Josephson Effects	13
2.6.4	Quantization of Magnetic Flux	13
2.7	Characteristics of the Superconducting State	14
2.7.1	Critical Magnetic Field	14
2.7.2	Critical Current Density	15
2.7.3	Penetration Depth and Coherence Length	16
2.8	Type I superconductors	18
2.9	Type II superconductors	19
2.9.1	Flux Pinning Mechanism in Type II Superconductor	20
2.9.2	The Mixed State	21
2.9.3	Vortex State	21
2.10	High-Temperature Superconductivity	22
2.10.1	Grain Boundary Problem	23
2.10.2	Grain Alignment	23
2.10.3	Pseudogap	24
2.10.4	Variation of T_c with Oxygen Stoichiometry	25

3	LITERATURE REVIEW	26
3.1	Yttrium-Barium Copper Oxide (YBCO) Ceramic Superconductor	26
3.2	Structure of $\text{YBa}_2\text{Cu}_3\text{O}_{7-\delta}$ Superconductor	26
3.3	Synthesis Methods of YBCO Superconducting Materials	27
3.3.1	Thermal Treatment Method	28
3.4	Studies on Y123 Superconductor Synthesised by the Thermal Treatment Method	29
3.5	Effect of CNT Addition on Y123 Bulk	31
3.6	Effect of TiO_2 Nanoparticles Addition on Y123 Bulk	33
3.7	Effect of SiC Nanoparticles Addition on Y123 Bulk	35
3.8	Effect of Addition of Various Nanoparticles on Y123 bulk	36
4	METHODOLOGY	44
4.1	Introduction	44
4.2	Materials used for This Research	44
4.2.1	Materials for Samples Preparation	44
4.2.2	Materials used as Addition	45
4.3	Sample Preparation	47
4.3.1	Nitrate Solution Preparation and Drying Process	47
4.3.2	Calcination Process	47
4.3.3	Pelletising and Sintering Process	49
4.4	Characterisation Techniques	51
4.4.1	Thermogravimetric Analysis (TGA)	51
4.4.2	X- Ray Diffraction Analysis (XRD)	51
4.4.3	Field Emission Scanning Electron Microscope (FESEM) and Energy Dispersive X- ray Spectrometer (EDX)	52
4.4.4	Alternating Current Susceptibility (ACS)	53
4.4.5	Four Probe Resistivity Measurement System	54
4.4.6	Electron-Spin Resonance (ESR)	55
5	RESULTS AND DISCUSSION	57
5.1	Introduction	57
5.2	Thermogravimetric Analysis (TGA)	57
5.3	X-ray Diffraction Analysis (XRD)	58
5.3.1	X-ray Diffraction Analysis for Pure Y123	58
5.3.2	Effect of CNT Addition	59
5.3.3	Effect of TiO_2 Addition	63
5.3.4	Effect of SiC Addition	66
5.4	Field Emission Scanning Electron Microscope (FESEM) Analysis	69
5.4.1	(FESEM) Analysis of Pure Y123	69
5.4.2	Effect of CNT Addition	70
5.4.3	Effect of TiO_2 Addition	76
5.4.4	Effect of SiC Addition	82
5.5	Energy Dispersive X- ray Spectrometer (EDX) Analysis	88
5.5.1	EDX Analysis of Pure Y123	88
5.5.2	EDX Analysis of Y123 with CNT Addition	90
5.5.3	EDX Analysis of Y123 with TiO_2 Addition	91

5.5.4	EDX Analysis of Y123 with SiC Addition	93
5.6	Alternating Current Susceptibility (ACS) Measurement	95
5.6.1	AC Susceptibility for Pure Y123	95
5.6.2	Effect of CNT Addition	98
5.6.3	Effect of TiO ₂ Addition	102
5.6.4	Effect of SiC Addition	110
5.7	Four-Point Probe Measurement	116
5.7.1	Resistivity of Pure Y123	116
5.7.2	Electrical Resistivity of Y123 with CNT Addition	119
5.7.3	Current-Voltage Characteristics and J_c Measurements	122
5.7.4	Electrical Resistivity for Y123 with TiO ₂ Addition	124
5.7.5	Electrical Resistivity for Y123 with SiC Addition	127
5.8	ESR Spectra Analysis	133
5.8.1	ESR Spectra for Pure Y123	133
5.8.2	ESR Spectra for Y123/CNT	134
5.8.3	ESR Spectra for Y123/TiO ₂	135
5.8.4	ESR Spectra for Y123/SiC	137
6	CONCLUSION AND FUTURE WORKS	140
6.1	Conclusion	140
6.2	Recommendations for Future Works	142
	REFERENCES	143
	APPENDICES	158
	BIODATA OF STUDENT	170
	LIST OF PUBLICATIONS	171

LIST OF TABLES

Table		Page
3.1	Y123 superconductor synthesised by using thermal treatment method from literature	39
3.2	Effect of CNT addition on Y123 bulk superconductor prepared via different methods from literature	40
3.3	Effect of TiO ₂ nanoparticles addition on Y123 bulk superconductor prepared via different methods from literature	41
3.4	Effect of SiC nanoparticles addition on Y123 bulk superconductor prepared via different methods from literature	42
3.5	Effect of different nanoparticles addition on Y123 bulk superconductor prepared via different methods from literature	43
4.1	Raw materials used to prepare Y123 ceramic by thermal treatment method	44
4.2	Some specifications of CNT, TiO ₂ and SiC nanostructures	46
5.1	Summary of lattice parameters <i>a</i> , <i>b</i> , and <i>c</i> , orthorhombicity, crystallite size, volume fraction and oxygen content for Y123 added with different amount of CNT (<i>x</i> = 0.0, 0.2, 0.4, 0.6, 0.8 and 1.0 wt.%)	63
5.2	Summary of lattice parameters <i>a</i> , <i>b</i> , and <i>c</i> , orthorhombicity, crystallite size, volume fraction and oxygen content for Y123 added with different amount of TiO ₂ (<i>x</i> = 0.0, 0.2, 0.4, 0.6, 0.8 and 1.0 wt.%)	66
5.3	Summary of lattice parameters <i>a</i> , <i>b</i> , and <i>c</i> , orthorhombicity, crystallite size, volume fraction and oxygen content for Y123 added with different amount of SiC (<i>x</i> = 0.0, 0.2, 0.4, 0.6, 0.8 and 1.0 wt.%)	69
5.4	EDX analysis of chemical composition of pure Y123	89
5.5	EDX analysis of chemical composition of Y123 with <i>x</i> = (0.2, 0.4, 0.6, 0.8 and 1.0 wt.%) CNT	91
5.6	EDX analysis of chemical composition of Y123 with <i>x</i> = (0.2, 0.4, 0.6, 0.8 and 1.0 wt.%) TiO ₂	93
5.7	EDX analysis of chemical composition of Y123 with <i>x</i> = (0.2, 0.4, 0.6, 0.8 and 1.0 wt.%) SiC	95

5.8	Summary data of $T_{c\text{-onset}}$, T_{cj} , T_p , $J_c(T_p)$, I_0 and, E_j of Y123/(CNT) x at $x = 0.0, 0.2, 0.4, 0.6, 0.8$ and 1.0 wt.%, measured at a magnetic field 0.5 Oe and a frequency of 219 Hz	102
5.9	Summary data of $T_{c\text{-onset}}$, T_{cj} , T_p , $J_c(T_p)$, I_0 and, E_j of Y123/(TiO ₂) x at $x = 0.0, 0.2, 0.4, 0.6, 0.8$ and 1.0 wt.%, measured at a magnetic field 5 Oe and a frequency of 295 Hz	110
5.10	Summary data of $T_{c\text{-onset}}$, T_{cj} , T_p , $J_c(T_p)$, I_0 and, E_j of Y123/(SiC) x at $x = 0.0, 0.2, 0.4, 0.6, 0.8$ and 1.0 wt.%, measured at a magnetic field 5 Oe and a frequency of 295 Hz	116
5.11	Properties of superconducting transition temperature ($T_{c\text{-onset}}$, $T_{c\text{-zero}}$, ΔT_c), residual resistivity, ρ_0 and hole concentration, p for Y123 at $x = 0.0, 0.2, 0.4, 0.6, 0.8, 1.0$ wt.% CNT addition	121
5.12	Properties of superconducting transition temperature ($T_{c\text{-onset}}$, $T_{c\text{-zero}}$, ΔT_c), residual resistivity, ρ_0 and hole concentration, p for Y123 at $x = 0.0, 0.2, 0.4, 0.6, 0.8,$ and 1.0 wt.% TiO ₂ addition	126
5.13	Properties of superconducting transition temperature ($T_{c\text{-onset}}$, $T_{c\text{-zero}}$, ΔT_c), residual resistivity, ρ_0 and hole concentration, p for Y123 at $x = 0.0, 0.2, 0.4, 0.6, 0.8,$ and 1.0 wt.% SiC addition	129
5.14	Summary of important results of T_c and J_c of Y123 with different amount of CNT, TiO ₂ and SiC addition from samples of this work compared to the samples of the literature	132
5.15	g-value, resonance field, H_r and peak-to-peak linewidth, ΔH_{pp} for Y123/(CNT) x , $x = 0.0, 0.2, 0.4, 0.6, 0.8,$ and 1.0 wt.%	135
5.16	g-value, resonance field, H_r and peak-to-peak linewidth, ΔH_{pp} for Y123/(TiO ₂) x , $x = 0.0, 0.2, 0.4, 0.6, 0.8$ and 1.0 wt.%	137
5.17	g-value, resonance field, H_r and peak-to-peak linewidth, ΔH_{pp} for Y123/(SiC) x , $x = 0.0, 0.2, 0.4, 0.6, 0.8,$ and 1.0 wt.%	138

LIST OF FIGURES

Figure		Page
1.1	Evolution of the superconducting transition temperature as a function of the year of discovery	3
2.1	Deformation of the lattice caused by the passage of an electron	8
2.2	Variation in the G-L free energy density as a function of the order parameter $ \psi ^2$ at different temperatures	9
2.3	The energy gap 2Δ at $T = 0$, and in a normal metal. The states below the gap are considered to be full and all those above it to be empty	10
2.4	The resistance of mercury measured by Onnes	11
2.5	The magnetic field lines for a superconductor: (a) the flux lines penetrate the sample (normal state), and (b) the shielding currents result in zero magnetic field inside the sample (Meissner state)	12
2.6	A magnet levitation experiment was conducted on a YBCO bulk sample in the laboratory of superconductor and thin film at UPM.	12
2.7	The magnetic flux inside (a) a superconducting cylinder (b) superconducting ring is an integral multiple of the flux quantum, $\Phi_0 = h/2e$	14
2.8	The boundary between the superconducting state and the normal state in the parabolic $H-T$ curve	15
2.9	Magnetic field penetration into a superconductor sample. The magnetic field drops off exponentially to zero inside the material	17
2.10	A comparison of λ and ξ in type I and type II superconductors	18
2.11	(a) Magnetisation as a function of applied magnetic field for type I superconductor. (b) Critical magnetic field versus temperature for type I superconductor	19
2.12	(a) Magnetisation as a function of applied magnetic field for type II superconductor. (b) Critical magnetic field versus temperature for type II superconductor	20
2.13	A type II superconductor undergoes mixed state between H_{c1} and H_{c2} . The material is penetrated by flux lines (Φ_0) produced by vortices of persistent current vortex that rotates in the opposite direction to surface screening current	21

2.14	A grain boundary with misorientation angle θ in the superconductor. If ξ is short the order parameter ψ reduces at the grain boundary	23
2.15	Phase diagram of high- T_c superconductor. The phase shows the pseudogap phase, the superconducting phase, and the antiferromagnetic (AF)	24
3.1	The Crystal structure of YBCO; (a) orthorhombic structure. (b) tetragonal structure.	27
3.2	A proposed mechanism of the interaction between PVP and metal ions	29
4.1	FESEM image shows the morphology feature of CNT powder	46
4.2	FESEM image shows the morphology feature of TiO_2 powder	46
4.3	FESEM image shows the morphology feature of SiC powder	47
4.4	Heating profiles for the first and second calcination processes	48
4.5	Heating profile for sintering process	49
4.6	Flow chart of preparation and characterisation of Y123 samples	50
4.7	Schematic diagram of XRD instrument	52
4.8	The diagram of the dimension used to determine the average grain size	53
4.9	Schematic diagram of the AC susceptibility measurement	54
4.10	Schematic diagrams of four-point probe technique	55
4.11	Spin state of energies as a function of a magnetic field	56
5.1	TGA/DTG curves for YBCO precursor gel prepared by thermal treatment method	58
5.2	X-Ray diffraction pattern of pure Y123 sample	59
5.3	X-Ray diffraction patterns of Y123 added with different amount of CNT ($x = 0.0, 0.2, 0.4, 0.6, 0.8$ and 1.0 wt.%)	60
5.4	A close-up view for the XRD patterns of the peaks related to the (013) and (103) planes of Y123 added with different amount of CNT ($x = 0.0, 0.2, 0.4, 0.6, 0.8$ and 1.0 wt.%)	61
5.5	The variation of lattice parameters a , b and c axis, and orthorhombicity of Y123 added with different amount of CNT ($x = 0.0, 0.2, 0.4, 0.6, 0.8$ and 1.0 wt.%)	62

5.6	X-Ray diffraction pattern of Y123 added with different amount of TiO ₂ ($x = 0.0, 0.2, 0.4, 0.6, 0.8$ and 1.0 wt.%)	64
5.7	The XRD patterns of the peaks related to the (013) and (103) planes of Y123 added with different amount of TiO ₂ ($x = 0.0, 0.2, 0.4, 0.6, 0.8$ and 1.0 wt.%)	64
5.8	Variation of lattice parameters a , b and c axis, and orthorhombicity of Y123 added with different amount of TiO ₂ ($x = 0.0, 0.2, 0.4, 0.6, 0.8$ and 1.0 wt.%)	65
5.9	X-Ray diffraction pattern of Y123 added with different amount of SiC ($x = 0.0, 0.2, 0.4, 0.6, 0.8$ and 1.0 wt.%)	67
5.10	The XRD patterns of the peaks related to the (013) and (103) planes of Y123 added with different amount of SiC ($x = 0.0, 0.2, 0.4, 0.6, 0.8$ and 1.0 wt.%)	67
5.11	Variation of lattice parameters a , b and c axis, and orthorhombicity of Y123 added with different amount of SiC	68
5.12	FESEM micrographs of pure Y123 of the surface morphology at magnifications (a) 10000x and (b) 50000x. (c) fractured bulk. (d) histogram of average grain size distribution	70
5.13	FESEM micrographs of Y123 with $x = 0.2$ wt.% CNT taken at surface morphology at magnifications (a) 10000x and (b) 50000x. (c) fractured bulk. (d) histogram of average grain size distribution	72
5.14	FESEM micrographs of Y123 with $x = 0.4$ wt.% CNT taken at surface morphology at magnifications (a) 10000x and (b) 50000x. (c) fractured bulk. (d) histogram of average grain size distribution	73
5.15	FESEM micrographs of Y123 with $x = 0.6$ wt.% CNT taken at surface morphology at magnifications (a) 10000x and (b) 50000x. (c) fractured bulk. (d) histogram of average grain size distribution	74
5.16	FESEM micrographs of Y123 with $x = 0.8$ wt.% CNT taken at surface morphology at magnifications (a) 10000x and (b) 50000x. (c) fractured bulk. (d) histogram of average grain size distribution	75
5.17	FESEM micrographs of Y123 with $x = 1.0$ wt.% CNT taken at surface morphology at magnifications (a) 10000x and (b) 50000x. (c) fractured bulk. (d) histogram of average grain size distribution	76
5.18	FESEM microstructure of Y123 with $x = 0.2$ wt.% TiO ₂ taken at surface morphology at magnifications (a) 3000x and (b) 25000x. (c) fractured bulk. (d) histogram of average grain size distribution	78

5.19	FESEM microstructure of Y123 with $x = 0.4$ wt.% TiO ₂ taken at surface morphology at magnifications (a) 3000x and (b) 25000x. (c) fractured bulk. (d) histogram of average grain size distribution	79
5.20	FESEM microstructure of Y123 with $x = 0.6$ wt.% TiO ₂ taken at surface morphology at magnifications (a) 3000x and (b) 25000x. (c) fractured bulk. (d) histogram of average grain size distribution	80
5.21	FESEM microstructure of Y123 with $x = 0.8$ wt.% TiO ₂ taken at surface morphology at magnifications (a) 3000x and (b) 25000x. (c) fractured bulk. (d) histogram of average grain size distribution	81
5.22	FESEM microstructure of Y123 with $x = 1.0$ wt.% TiO ₂ taken at surface morphology at magnifications (a) 3000x and (b) 25000x. (c) fractured bulk. (d) histogram of average grain size distribution	82
5.23	FESEM microstructure of Y123 with $x = 0.2$ wt.% SiC taken at surface morphology at magnifications (a) 3000x and (b) 25000x. (c) fractured bulk. (d) histogram of average grain size distribution	84
5.24	FESEM microstructure of Y123 with $x = 0.4$ wt.% SiC taken at surface morphology at magnifications (a) 3000x and (b) 25000x. (c) fractured bulk. (d) histogram of average grain size distribution	85
5.25	FESEM microstructure of Y123 with $x = 0.6$ wt.% SiC taken at surface morphology at magnifications (a) 3000x and (b) 25000x. (c) fractured bulk. (d) histogram of average grain size distribution	86
5.26	FESEM microstructure of Y123 with $x = 0.8$ wt.% SiC taken at surface morphology at magnifications (a) 3000x and (b) 25000x. (c) fractured bulk. (d) histogram of average grain size distribution	87
5.27	FESEM microstructure of Y123 with $x = 1.0$ wt.% SiC taken at surface morphology at magnifications (a) 3000x and (b) 25000x. (c) fractured bulk. (d) histogram of average grain size distribution	88
5.28	Typical (EDX) spectrums of pure Y123 performed at full area (a, b) and points (c, d)	89
5.29	(a-e) (EDX) spectrums of Y123 with the addition of CNT, $x = (0.2, 0.4, 0.6, 0.8$ and 1.0 wt.%), respectively	90
5.30	(a-f) Electron image and EDX of elemental mapping distribution of Y, B, C, O and C ions, respectively at $x = 0.4$ wt.% CNT addition	91
5.31	(a-e) (EDX) spectrums of Y123 with the addition of TiO ₂ , $x = (0.2, 0.4, 0.6, 0.8$ and 1.0 wt.%), respectively	92
5.32	(a-f) Electron image and EDX of elemental mapping distribution of Y, B, C, O and Ti ions, respectively at $x = 0.6$ wt.% TiO ₂ addition	93

5.33	(a-e) (EDX) spectrums of Y123 with the addition of SiC, $x = (0.2, 0.4, 0.6, 0.8 \text{ and } 1.0 \text{ wt.}\%)$, respectively	94
5.34	(a-f) Electron image and EDX of elemental mapping distribution of Y, B, C, O and Si ions, respectively at $x = 0.6 \text{ wt.}\%$ SiC addition	95
5.35	AC susceptibility ($\chi = \chi' + i\chi''$) versus temperature of pure Y123 measured at magnetic field amplitude 0.5 Oe and frequency 219 Hz	97
5.36	Derivative of the real part of AC susceptibility, $d\chi'/dT$ as a function of temperature for pure Y123 measured at magnetic field amplitude 0.5 Oe and frequency 219 Hz	97
5.37	AC susceptibility ($\chi = \chi' + i\chi''$) versus temperature of Y123/(CNT) $_x$ at $x = 0.0, 0.2, 0.4, 0.6, 0.8 \text{ and } 1.0 \text{ wt.}\%$, measured at a magnetic field 0.5 Oe and a frequency of 219 Hz	98
5.38	Derivative of the real part of AC susceptibility, $d\chi'/dT$ as a function of temperature of Y123/(CNT) $_x$ at $x = 0.0, 0.2, 0.4, 0.6, 0.8 \text{ and } 1.0 \text{ wt.}\%$	99
5.39	Real curves of AC susceptibility versus temperature, (χ' -T) of Y123/(CNT) $_x$ at $x = 0.0, 0.2, 0.4, 0.6, 0.8 \text{ and } 1.0 \text{ wt.}\%$, measured at a magnetic field 0.5 Oe and a frequency of 219 Hz	100
5.40	Imaginary curves of AC susceptibility versus temperature (χ'' -T) of Y123/(CNT) $_x$ at $x = 0.0, 0.2, 0.4, 0.6, 0.8 \text{ and } 1.0 \text{ wt.}\%$, measured at a magnetic field 0.5 Oe and a frequency 219 Hz	101
5.41	AC susceptibility ($\chi = \chi' + i\chi''$) versus temperature of pure Y123 measured at a magnetic field 5 Oe and a frequency of 295 Hz	103
5.42	Derivative of the real part of AC susceptibility, $d\chi'/dT$ as a function of temperature for pure Y123 measured at a magnetic field 5 Oe and a frequency of 295 Hz	103
5.43	AC susceptibility ($\chi = \chi' + i\chi''$) versus temperature of Y123/(TiO ₂) $_x$ at $x = 0.0, 0.2, 0.4, 0.6, 0.8 \text{ and } 1.0 \text{ wt.}\%$, measured at a magnetic field 5 Oe and a frequency of 295 Hz	104-106
5.44	Derivative of the real part of AC susceptibility, $d\chi'/dT$ as a function of temperature of Y123/(TiO ₂) $_x$ at $x = 0.0, 0.2, 0.4, 0.6, 0.8 \text{ and } 1.0 \text{ wt.}\%$	107
5.45	Real curves of AC susceptibility versus temperature, (χ' -T) of Y123/(TiO ₂) $_x$ at $x = 0.0, 0.2, 0.4, 0.6, 0.8 \text{ and } 1.0 \text{ wt.}\%$, measured at a magnetic field 5 Oe and a frequency of 295 Hz	108
5.46	Imaginary curves of AC susceptibility versus temperature (χ'' -T) of Y123/(TiO ₂) $_x$ at $x = 0.0, 0.2, 0.4, 0.6, 0.8 \text{ and } 1.0 \text{ wt.}\%$, measured at a magnetic field 5 Oe and a frequency of 295 Hz	109

5.47	AC susceptibility ($\chi = \chi' + i\chi''$) versus temperature of Y123/(SiC) $_x$ at $x = 0.0, 0.2, 0.4, 0.6, 0.8$ and 1.0 wt.%, measured at a magnetic field 5 Oe and a frequency of 295 Hz	111- 113
5.48	Derivative of the real part of AC susceptibility, $d\chi'/dT$ as a function of temperature of Y123/(SiC) $_x$ at $x = 0.0, 0.2, 0.4, 0.6, 0.8$ and 1.0 wt.%	113
5.49	Real curves of AC susceptibility versus temperature, ($\chi'-T$) of Y123/(SiC) $_x$ at $x = 0.0, 0.2, 0.4, 0.6, 0.8$ and 1.0 wt.%, measured at a magnetic field 5 Oe and a frequency of 295 Hz	114
5.50	Imaginary curves of AC susceptibility versus temperature ($\chi''-T$) of Y123/(SiC) $_x$ at $x = 0.0, 0.2, 0.4, 0.6, 0.8$ and 1.0 wt.%, measured at a magnetic field 5 Oe and a frequency of 295 Hz	115
5.51	Resistivity versus temperature curve of pure Y123	118
5.52	The derivative of resistivity against temperature curve of pure Y123	118
5.53	Temperature dependent resistivity of Y123 at $x = 0.0, 0.2, 0.4, 0.6, 0.8, 1.0$ wt.% CNT addition	119
5.54	The derivative of resistivity against temperature curves for Y123 at $x = 0.0, 0.2, 0.4, 0.6, 0.8, 1.0$ wt.% CNT addition	120
5.55	Comparison curves of T_{c-zero} , T_{c-zero} and p of Y123 at $x = 0.0, 0.2, 0.4, 0.6, 0.8, 1.0$ wt.% CNT addition	121
5.56	(a-f): I-V curves for Y123 with various wt.% CNT addition at $x = 0.0, 0.2, 0.4, 0.6, 0.8,$ and 1.0	123
5.57	Variation of critical current density J_c with different concentration of wt.% CNT addition at $x = 0.0, 0.2, 0.4, 0.6, 0.8,$ and 1.0	124
5.58	Temperature dependent resistivity of Y123 at $x = 0.0, 0.2, 0.4, 0.6, 0.8,$ and 1.0 wt.% TiO ₂ addition	125
5.59	The derivative of resistivity against temperature curves for Y123 at $x = 0.0, 0.2, 0.4, 0.6, 0.8,$ and 1.0 wt.% TiO ₂ addition	126
5.60	Comparison of $T_{c-onset}$, T_{c-zero} and p curves of Y123 at $x = 0.0, 0.2, 0.4, 0.6, 0.8,$ and 1.0 wt.% TiO ₂ addition	127
5.61	Temperature dependent resistivity of Y123 at $x = 0.0, 0.2, 0.4, 0.6, 0.8,$ and 1.0 wt.% SiC addition	128
5.62	The derivative of resistivity against temperature curves for Y123 at $x = 0.0, 0.2, 0.4, 0.6, 0.8,$ and 1.0 wt.% SiC addition	129

5.63	Comparison of $T_{c-onset}$, T_{c-zero} and p curves of Y123 at $x = 0.0, 0.2, 0.4, 0.6, 0.8,$ and 1.0 wt.% SiC addition	130
5.64	Comparison of $T_{c-onset}$ of Y123 with different amount of CNT, TiO_2 and SiC addition at $x = 0.0, 0.2, 0.4, 0.6, 0.8,$ and 1.0 wt.%	131
5.65	ESR spectra pattern of pure Y123 sample measured at room temperature	133
5.66	ESR spectra pattern of Y123 at $x = 0.0, 0.2, 0.4, 0.6, 0.8$ and 1.0 wt.% CNT addition measured at room temperature	135
5.67	(a) ESR spectra pattern of Y123 at $x = 0.0, 0.2, 0.4, 0.6, 0.8,$ and 1.0 wt.% TiO_2 addition, measured at room temperature. (b) The inset details of ESR patterns for samples at $x = (0.4 - 1.0)$	136
5.68	ESR spectra pattern of Y123 at $x = 0.0, 0.2, 0.4, 0.6, 0.8,$ and 1.0 wt.% SiC addition measured at room temperature	138

LIST OF ABBREVIATIONS

A	Ampere
Å	Angstrom
AC	Alternating current
ACS	Alternating Current Susceptibility
<i>a, b, c</i> axis	Lattice parameters
B	Magnetic field
BCS	(Bardeen-Cooper-Schrieffer) Theory
BSCCO	Bismuth lead strontium calcium copper oxide
°C	Degree Celsius
CNT	Carbon nanotube
DC	Direct current
d_p	Crystallite size
DTG	Derivative Thermogravimetric Analysis
EDX	Energy dispersive x-ray Analysis
ESR	Electron-spin resonance
FESEM	Field emission scanning electron microscopy
F_L	Lorentz force
f_s	Free energy in the normal state
FWHM	Full width half maximum
G-L	Ginzburg-Landau theory
h	Hour
H_{ac}	Applied field
H_{c1}	Lower critical field
H_{c2}	Upper critical field
HTSC	High temperature superconductor
Hz	Hertz
I	Current

I_0	Critical Josephson current
ICDD	International Centre for Diffraction Data
J_c	Critical current density
J_{cm}	Intergranular critical current density
K	Kelvin
La-Ba-Cu-O	lanthanum barium copper oxides
LTS	low temperature superconductor
MgB ₂	Magnesium diboride
min	Minute
mm	Millimetre
nm	Nanometre
Oe	Oersted
P	Hole concentration
PVP	Polyvinyl pyrrolidone
R	Resistance
rpm	Rotation per minute
sec	Second
SiC	Silicon carbide
SQUID	Superconducting quantum interference device
T^*	Pseudogap temperature
TBCCO	Thallium barium calcium copper oxide
T_c	Critical temperature
T_{cj}	Phase lock-in temperature
$T_{c-onset}$	Onset critical temperature
T_{c-zero}	Transition temperature at zero resistivity
TGA	Thermogravimetric Analysis
TiO ₂	Titanium Oxide
T_p	Coupling peak temperature
T_{pm}	Intergranular peak temperature
T_{pg}	Intragranular peak temperature

V	Voltage
wt.%	Weight percentage
XRD	X-ray diffraction
$\text{YBa}_2\text{Cu}_3\text{O}_{7-\delta}$ (YBCO, Y123)	Yttrium barium copper oxide
Y211	Y_2BaCuO_5
Y124	$\text{YBa}_2\text{Cu}_4\text{O}_8$
Y247	$\text{Y}_2\text{Ba}_4\text{Cu}_7\text{O}_{15}$
ΔT_c	Transition width
ρ	Electrical resistivity
ρ_0	Residual resistivity
$\rho-T$	Resistivity-temperature measurement
χ'	Real part of ACS
χ''	Imaginary Part of ACS
ψ	Order parameter
κ	Ginzburg-Landau constant
ϕ	Phase of the order parameter
Φ_0	Quantum of flux
λ	Penetration depth
ξ	Coherence length
δ	Oxygen deficiency
θ	Angle of the diffracted
Ω	Ohm
μm	Micrometre

CHAPTER 1

INTRODUCTION

1.1 Superconducting Phenomenon: its Discovery and Evolution

The phenomenon of superconductivity was first discovered in 1911 by H. Kamerlingh Onnes and Gilles Holst, who found that at a temperature below 4.2 K, the dc resistivity of mercury abruptly drops to zero. At this point, the transition temperature, T_c , between the normal and superconducting states is the first quantity used to characterise a superconducting material. This temperature is also known as the critical temperature. Walther Meissner and Robert Ochsenfeld discovered in 1933 that a magnetic field is expelled from the inside of a material cooled down below its critical temperature when superconductors are exposed to an external magnetic field (Forrest, 1983). Thus, no applied magnetic field is permitted inside when metal becomes superconducting. This phenomenon is one of the most fundamental properties of superconductors and is referred to as the Meissner effect.

In 1934, Dutch scientists C. J. Gorter and H. B. G. Casimir proposed a phenomenological explanation of superconductivity based on the idea that the conducting electron "fluid" has two components: normal and superconducting in the superconducting state. Electrons with normal properties are identical to the electron system in a normal metal, whereas superconducting electrons are the cause of the anomalous features. In 1935, following the discovery of the Meissner effect, the brothers F. and H. London introduced two equations to explain the diamagnetism of superconductors in a weak external field. The London equations defined the first characteristic length of superconductivity, which is now referred to as the London penetration depth L . The London equations, along with the Maxwell equations, explained the behaviour of superconducting electrons within the framework of the two-fluid model. In contrast, the Maxwell equations only described the behaviour of normal electrons.

The presence of two critical magnetic fields for type-II superconductors and the mixed state was discovered in 1937 by L. V. Shubnikov and co-workers. Actually, they discovered vortices in superconductors. The isotope effect in superconductors was found by E. Maxwell and C. A. Reynolds in 1950. This finding was essential to establishing the correct theory of superconductivity. The phenomenological theory of superconductivity that uses the second-order phase transition theory was proposed by Ginzburg and Landau in the same year, 1950. The Ginzburg-Landau theory was able to explain how superconductors, both conventional and unconventional, react when subjected to intense magnetic fields. The Ginzburg-Landau theory offered an expression for the coherence length, which is the second characteristic length of superconductivity.

Cooper, (1956) showed that if two conducting experience an attractive interaction on the Fermi surface, they will form a stable paired state. A pair like these is known as a Cooper

pair. Based on these findings, J. Bardeen, L. Cooper, and R. Schrieffer (Abrikosov, 1957) developed the first microscopic theory in 1957, which is now widely known as the BCS theory. Following BCS, B. D. Josephson predicted research on tunnelling effects between two bulk superconductors separated by an insulating barrier (a few nanometres thick) (Josephson, 1962). Within a year, the predictions of Josephson were confirmed, and they became known as the Josephson effects.

1.2 High-Temperature Superconductivity (HTSC): A history

The history of high-temperature superconductivity started in late 1986, when George Bednorz and Karl Müller observed evidence for superconductivity in lanthanum barium copper oxides (La-Ba-Cu-O) ceramics at temperatures up to 38 K (Bednorz et al., 1986). In 1987, scientists at the Universities of Alabama and Houston, led by Wu and Chu, jointly announced the finding of the 93 K superconductor in yttrium barium copper oxide (Y-Ba-Cu-O) (Wu et al., 1987). The focus then turned to copper oxides, and shortly after, the compounds BSCCO with $T_c = 105$ K and TBCCO with $T_c = 125$ K were discovered in 1988 (Maeda et al., 1988; Sheng et al., 1988). In 1993, the highest critical temperature, $T_c = 135$ K for Hg-based cuprates ($\text{HgBa}_2\text{Ca}_2\text{Cu}_3\text{O}_x$) was observed (Chu et al., 1993). The T_c for the mercury compounds can reach 164 K at high pressure (Sheng et al., 1988).

Figure 1.1 shows the evolution of the transition temperature, T_c , of different cuprate superconductors. The figure includes the metallic compound MgB_2 and the iron group. Meanwhile, the MgB_2 compound was discovered in 2000 with a transition temperature of 39 K (Nagamatsu et al., 2001). The physics community was highly active as a result of this discovery, and significant characteristics of this substance were determined over the next two years. Comparable to the "classical" metallic superconductors, MgB_2 exhibits similar characteristics. In 2008, an iron pnictide with transition temperatures as high as 56 K was discovered (Takahashi et al., 2008).

The mechanism by which high-temperature superconductors achieve their properties is still the topic of discussion. The data collected in the cuprates within a year of their superconducting discovery showed that the features of high- T_c superconductors varied from those predicted by the BCS theory. The BCS isotope effect, for example, is almost non-existent in optimally doped cuprates. This has resulted in the development of the mechanisms of non-phonon electronic coupling. Within the past several years, bulk HTSC that have large critical currents, high trapped fields, and powerful levitation forces have been developed. This development in bulk HTSC growth was particularly noticeable for the $\text{YBa}_2\text{Cu}_3\text{O}_{7-\delta}$ or (Y123) compound, which plays a major role in applications of superconducting materials. The Y123 is one of the most promising high- T_c superconductors for applications at 77 K due to its relatively small anisotropy, which enables large critical current densities even when applied magnetic fields are present. The highest T_c value for $\text{YBa}_2\text{Cu}_3\text{O}_{7-\delta}$ is 93 K at $\delta = 0.1$. It has been found that if Y is substituted by another rare-earth element, such as Nd, Eu, Gd, Er, Sm, Dy, Tm, or Ho, the resulting T_c is essentially unaffected.

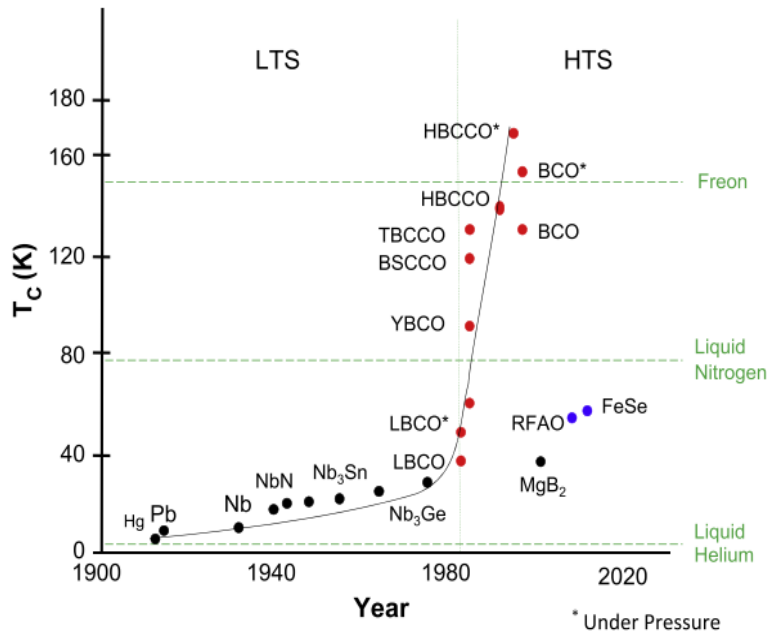


Figure 1.1: Evolution of the superconducting transition temperature as a function of the year of discovery (Chu et al., 2015)

1.3 Applications of High- T_c Superconductors

As soon as high- T_c superconductors were discovered, it was realised that significant economic savings would be possible using liquid nitrogen rather than liquid helium (low temperature superconductor LTS such as NbTi and Nb₃Sn). HTSC will contribute significantly to energy savings and greenhouse gas reductions when novel designs of power components and systems become available. The commercial applications of HTSC became increasingly fascinating after their discovery. Indeed, superconductor wire's electrical efficiency and great power density result in powerful and highly compact devices that are more dependable, efficient, and environmentally friendly. Hence, their applications include various areas such as medical, transportation, electrical grids, and industry. The most advanced HTSC used in power systems are power transmission cables. In fact, 2001 has proven to be a pivotal year for HTSC cable prototypes, with important pre-commercial demonstrations taking place on many continents, some of which are supplying electricity for commercial and residential usage (Hassenzahl, 2001; Kelley et al., 2001).

The diamagnetic property of bulk HTSC superconductors has been employed to produce levitators and bearings (Hull, 2000). Because bulk HTSC can effectively trap magnetic fields, they are worth seriously considering for usage in power generation. Bulk HTSC have been used to generate a trapped field of 17 T at 29 K, with the value being restricted by the strength of the energising magnet (Tomita & Murakami, 2003). The development

of HTSC motors started soon after they were discovered (Driscoll et al., 2000). This effort led to the creation of experimental devices with ever-growing sizes. Bulk HTSC motors have lately been studied as analogues to reluctance (Oswald et al., 1999) and hysteresis (Kovalev et al., 1999) permanent-magnet motors. For generator applications, it is expected that HTSC generators will make it possible to compete at 100 MVA and higher because of the greater temperature cooling related to HTSC (Rabinowitz, 2000). Superconducting bulk YBCO has been employed as a bearing system in a flywheel device to store power with a capacity of about 1 kW/h (Hull, 1997). Another application for bulk YBCO is water cleaning by magnetic separation technology (Hayashi et al., 2003). The high critical temperature and high current density of YBCO thin films make it ideal for use in small superconducting devices.

1.4 Problem Statement

The promise of superconductivity to revolutionise power applications has been there since its discovery. The interest in using superconductors in power technology was renewed by the discovery of a material that could superconduct at temperatures higher than the boiling point of liquid nitrogen. Materials with a high critical current density, J_c , and minimal power losses are crucial for bulk applications.

The major problem that has stood in the way of using Y123 bulk superconductors in technological applications is that these materials tend to have a granular consistency. This characteristic leads to weak flux pinning at the boundaries of the grains, which results in lowering J_c , causing the materials to lose its superconducting properties at high magnetic fields. (Bishop et al., 1992; Larbalestier, 1996; Tanaka, 2006). It is necessary to find a way to strength the weak flux pinning of Y123 materials to make it suitable for high magnetic field applications.

The beneficial way to enhance the weak flux pinning and superconducting properties with stabilising T_c is by introducing suitable impurities within the structure of the superconducting system. In addition, to ensure the effectiveness of the pinning centres, the size of the pinning should be on the order of the coherence length (distance over which the two electrons in the Cooper pair can bond) (Hari Babu et al., 2006; Yang & Wang, 2013). The presence of nano-sized impurity phases as defects in Y123 superconductor can act as artificial pinning centers to enhance its superconducting properties. (Lian et al., 1990; Ochsenkühn-Petropoulou et al., 2002; Rodriguez & Lazo, 2018; Wei et al., 2016; Xu et al., 2012; Xu et al., 2002). Hence, the aim of this research is to study the addition of CNT, TiO₂, and SiC nanostructures to Y123 via the thermal treatment method and investigate their potential to enhance weak flux pinning and superconducting performance. While various studies have investigated Y123 superconductors' performance enhancement through different synthesis methods, none have applied the thermal treatment method to introduce CNT, TiO₂, and SiC into the Y123 matrix. The current challenge lies in the lack of reported studies employing this synthesis method to introduce these specific nanostructures into Y123. It is expected that the structure and related superconducting properties of the Y123 superconductor will be enhanced when an adequate amount of impurity is introduced to the Y123 system using thermal treatment method. The role of the incorporation of different amounts of CNT,

TiO₂, and SiC into the microstructure and superconducting properties of Y123 bulk was thoroughly investigated and discussed.

1.5 Research Objectives

The following is a summary of the objectives for this research:

1. To synthesis a good quality of Y123 bulk superconductor using the thermal treatment method with PVP as a capping agent and determine its structure and superconducting properties.
2. To study the effect of the distribution of different percentages of CNT, TiO₂ and SiC nano powders on phase formation, microstructural and morphology of Y123 bulk.
3. To investigate the influence of CNT, TiO₂ and SiC nano powders addition on the electrical, magnetic, and superconducting properties of Y123 bulk.

1.6 Outline of the Thesis

The thesis is organised into six chapters, as follows: In Chapter 1, significant historical events connected to the phenomenon of superconductivity are reviewed. This chapter also presents a historical overview of high temperature superconductivity and its applications. The problem statement, objectives of the research, and outline of the thesis are given in this chapter. Chapter 2 explains the basic theories of superconductivity and discusses the fundamental properties of superconductors. The following topics are covered in this chapter: The BCS, zero electrical resistivity, the Meissner-Ochsenfeld effect, the Josephson effects, quantisation of magnetic flux, critical magnetic field, critical current density, penetration depth, and coherence length, type-I and type-II superconductors, flux pinning mechanism in type II superconductors, the mixed state, the vortex state, grain boundary problem, grain alignment, the pseudogap and variation of T_c with oxygen stoichiometry. Chapter 3 gives an overview of the literature review on the Y123 superconductor prepared by the thermal treatment method and the effect of the addition of CNT, TiO₂, and SiC nano powder on the Y123 system. The preparation method and sample characterisation techniques are presented in Chapter 4. The following chapter, Chapter 5, went over the results and discussed crystal structure, morphological, elemental distribution, AC susceptibility measurement, electrical resistivity and ESR spectra analysis. Finally, the outcomes that can be derived from this study are summarised in Chapter 6.

REFERENCES

- Abbasi, H., Taghipour, J., & Sedghi, H. (2010). Superconducting and transport properties of (Bi-Pb)-Sr-Ca-Cu-O with Cr₂O₃ additions. *Journal of Alloys and Compounds*, 494(1–2), 305–308.
- Abd-Ghani, S. N., Wye, H. K., Kong, I., Abd-Shukor, R., & Kong, W. (2014). Enhanced transport critical current density of NiO nano particles added YBCO superconductors. *In Advanced Materials Research*, 895, 105–108.
- Abdulhayi, A., Gholap, A. V., & Abd-Shukor, R. (2019). Effect of Different Nano-sized MgO Addition on YBa₂Cu₃O_{7-δ} Superconductor. *Journal of Superconductivity and Novel Magnetism*, 32(9), 2837–2847.
- Abrikosov, A. A. (1957). On the magnetic properties of superconductors of the second group. *Soviet Journal of Experimental and Theoretical Physics*, 5, 1174–1182.
- Alhassan, W. A. A., & Ismail, H. G. (2014). Determination of energy gap copper oxide by four probe methods. *International Journal of Renewable Energy Technology Research*, 3, 1–8.
- Ali, A., Nadiyah, A., & Auli, N. A. (2020). Comparison between solid state reaction and coprecipitation method of titanium oxide addition on the YBa₂Cu₃O₈ ceramics. *Materials Science Forum*, 1010, 187–193.
- Alotaibi, S. A., Slimani, Y., Hannachi, E., Almessiere, M. A., Yasin, G., Al-qwairi, F. O., Iqbal, M., & Ben Azzouz, F. (2021). Intergranular properties of polycrystalline YBa₂Cu₃O_{7-δ} superconductor added with nanoparticles of WO₃ and BaTiO₃ as artificial pinning centers. *Ceramics International*, 47(24), 34260–34268.
- Ambegaokar, V., & Baratoff, A. (1963). Tunneling between superconductors. *Physical Review Letters*, 10(11), 486.
- Arlina, A., Halim, S. A., Kechik, M. M. A., & Chen, S. K. (2015). Superconductivity in Bi-Pb-Sr-Ca-Cu-O ceramics with YBCO as additive. *Journal of Alloys and Compounds*, 645, 269–273.
- Aslamazov, L. G., Larkin, A. I., Ovchinnikov, Y. N., & Fiz, Z. (1969). Josephson Effect in Superconductors Separated by a Normal Metal. *Soviet Journal of Experimental and Theoretical Physics*, 28(1), 171.
- Awana, V. P. S., Malik, S. K., Yelon, W. B., Cardoso, C. A., de Lima, O. F., Gupta, A., Sedky, A., & Narlikar, A. v. (2000). Neutron diffraction on Er_{1-x}Ca_xBa₂Cu₃O_{7-δ} (0.0 ≤ x ≤ 0.3) system: Possible oxygen vacancies in Cu-O₂ planes. *Physica C: Superconductivity*, 338(3), 197–204.
- Awano, M., Fujishiro, Y., Moon, J., Takagi, H., Rybchenko, S., & Bredikhin, S. (2000). Microstructure control of an oxide superconductor on interaction of pinning

centers and growing crystal surface. *Physica C: Superconductivity*, 341–348, 2017–2018.

- Bahboh, A., Shaari, A. H., Baqiah, H., Kean, C. S., Kechik, M. M. A., Talib, Z. A., & Dihom, M. M. (2019). Effect of sol-gel synthesized BiFeO₃ nanoparticle addition in YBa₂Cu₃O_{7-δ} (Y123) superconductor synthesized by standard solid state reaction method. *Solid State Phenomena*, 290, 245–251.
- Barboux, P., Tarascon, J. M., Greene, L. H., Hull, G. W., & Bagley, B. G. (1988). Bulk and thick films of the superconducting phase YBa₂Cu₃O_{7-y} made by controlled precipitation and sol-gel processes. *Journal of Applied Physics*, 63(8), 2725–2729.
- Bardeen, J., Cooper, L. N., & Schrieffer, J. R. (1957a). Microscopic theory of superconductivity. *Physical Review*, 106(1), 162.
- Bardeen, J., Cooper, L. N., & Schrieffer, J. R. (1957b). Theory of superconductivity. *Physical Review*, 108(5), 1175–1204.
- Bean, C. P. (1964). Magnetization of High-Field Superconductors. *Reviews of Modern Physics*, 36(1), 31.
- Bednorz, J. G., & Müller, K. A. (1986). Possible High *T_c* Superconductivity in the Ba-La-Cu-O System. *Zeitschrift für Physik B Condensed Matter*, 64(2), 189–193.
- Beno, M.A., Soderholm, L., Capone, D.W., Hinks, D.G., Jorgensen, J.D., Grace, J.D., Schuller, I.K., Segre, C.U. and Zhang, K. (1987). Structure of the single-phase high-temperature superconductor YBa₂Cu₃O_{7-δ}. *Applied Physics Letters*, 51(1), 57–59.
- Benzi, P., Bottizzo, E., & Rizzi, N. (2004). Oxygen determination from cell dimensions in YBCO superconductors. *Journal of Crystal Growth*, 269(2–4), 625–629.
- Bertand, D. (2005). A Relativistic BCS Theory of Superconductivity. PhD Thesis, Universit'e catholique de Louvain.
- Bhattacharya, R. N., & Paranthaman, M. P. (Eds.). (2011). *High temperature superconductors*. Weinheim: John Wiley & Sons.
- Bishop, D. J., Gammel, P. L., Huse, D. A., & Murray, C. A. (1992). Magnetic flux-line lattices and vortices in the copper oxide superconductors. *Science*, 255(5041), 165–172.
- Bohandy, J., Suter, J., Kim, B. F., Moorjani, K., & Adrian, F. J. (1987). Gamma radiation resistance of the high *T_c* superconductor YBa₂Cu₃O_{7-δ}. *Applied Physics Letters*, 51(25), 2161–2163.
- Brecht, E., Schmahl, W. W., Mieke, G., Rodewald, M., Fuess, H., Andersen, N. H., Hanßmann, J., & Wolf, T. (1996). Thermal treatment of YBa₂Cu_{3-x}Al_xO_{6+δ} single crystals in different atmospheres and neutron-diffraction study of excess oxygen

pinned by the Al substituents. *Physica C: Superconductivity and Its Applications*, 265(1–2), 53–66.

- Campbell, A. M., & Evetts, J. E. (1972). Flux vortices and transport currents in type II superconductors. *Advances in Physics*, 21(90), 199–428.
- Campbell, A. M. (1995). AC Losses in High T_c Superconductors. *IEEE Transactions on Applied Superconductivity*, 5(2), 682–687.
- Cao, S., Li, L., Liu, F., Li, W., Chi, C., Jing, C., & Zhang, J. (2005). Structure and charge transfer correlated with oxygen content for a $Y_{0.8}Ca_{0.2}Ba_2Cu_3O_y$ ($y = 6.84-6.32$) system: A positron study. *Superconductor Science and Technology*, 18(5), 606–610.
- Cava, R. J., Batlogg, B., Chen, C. H., Rietman, E. A., Zahurak, S. M., & Werder, D. (1987). Oxygen stoichiometry, superconductivity and normal-state properties of $YBa_2Cu_3O_{7-\delta}$. *Nature*, 329(6138), 423–425.
- Cava, R. J., Hewat, A. W., Hewat, E. A., Batlogg, B., Marezio, M., Rabe, K. M., Krajewski, J. J., Peck, W. F., & Rupp, L. W. (1990). Structural anomalies, oxygen ordering and superconductivity in oxygen deficient $Ba_2YCu_3O_x$. *Physica C: Superconductivity and Its Applications*, 165(5–6), 419–433.
- Chaddah, P. (2003). Critical current densities in superconducting materials. *Sadhana - Academy Proceedings in Engineering Sciences*, 28(1–2), 273–282.
- Chaillout, C., Alario-Franco, M. A., Capponi, J. J., Chenavas, J., Strobel, P., & Marezio, M. (1988). Oxygen vacancy ordering in $Ba_2YCu_3O_{7-x}$ around $x = 0.5$. *Solid State Communications*, 65(4), 283–286.
- Chamekh, S., & Bouabellou, A. (2018). The Effects of Magnetic Dopant on the Structural and Electrical Properties in Superconducting $YBa_2Cu_3O_{7-\delta}$ Ceramic. *Advances in Chemical Engineering and Science*, 28(1–2), 273–282.
- Chisholm, M. F., & Pennycook, S. J. (1991). Structural origin of reduced critical currents at $YBa_2Cu_3O_{7-\delta}$ grain boundaries. *Nature*, 351(6321), 47–49.
- Chu, C. W. (1987). Superconductivity above 90 K. *Proceedings of the National Academy of Sciences*, 84(14), 4681–4682.
- Chu, C. W., Gao, L., Chen, F., Huang, Z. J., Meng, R. L., & Xue, Y. Y. (1993). Superconductivity above 150 K in $HgBa_2Ca_2Cu_3O_{8+\delta}$ at high pressures. *Nature*, 365(6444), 323–325.
- Chu, C. W., Deng, L. Z., & Lv, B. (2015). Hole-doped cuprate high temperature superconductors. *Physica C: Superconductivity and Its Applications*, 514, 290–313.

- Çiçek, Ö., & Yakinci, K. (2020). Enhanced superconducting properties of multi-wall carbon nanotubes added YBCO-123 Superconducting System. *Journal of Molecular Structure*, 1211, 128089.
- Clem, J. R. (1988). Granular and superconducting-glass properties of the high-temperature superconductors. *Physica C: Superconductivity*, 153, 50–55.
- Cooper, L. N. (1956). Bound electron pairs in a degenerate Fermi gas. *Physical Review*, 104(4), 1189.
- Cui, X. M., Tao, B. W., Xiong, J., Liu, X. Z., & Li, Y. R. (2005). YBCO superconducting film coated on LaAlO₃ substrate by TFA-MOD process. *Journal of Superconductivity and Novel Magnetism*, 18(2), 291–294.
- Cyrot, M. (1973). Ginzburg-Landau theory for superconductors. *Reports on Progress in Physics*, 36, 103–158.
- Dadras, S., Liu, Y., Chai, Y. S., Daadmehr, V., & Kim, K. H. (2009). Increase of critical current density with doping carbon nano-tubes in YBa₂Cu₃O_{7-δ}. *Physica C: Superconductivity and Its Applications*, 469(1), 55–59.
- Dadras, S., & Gharehgazloo, Z. (2016a). Effect of Au nano-particles doping on polycrystalline YBCO high temperature superconductor. *Physica B: Condensed Matter*, 492, 45–49.
- Dadras, S., & Ghavamipour, M. (2016b). Investigation of the properties of carbon-base nanostructures doped YBa₂Cu₃O_{7-δ} high temperature superconductor. *Physica B: Condensed Matter*, 484, 13–17.
- Dadras, S., Davoudiniya, M., & Dehghani, S. (2017). Investigation and Comparing the Effects of CNTs and Ag Nanoparticles Doping on YBCO Superconductor Properties. *Journal of Superconductivity and Novel Magnetism*, 30(9), 2451–2456.
- Dadras, S., & Davoudiniya, M. (2018). Analysis of YBCO high temperature superconductor doped with silver nanoparticles and carbon nanotubes using Williamson–Hall and size–strain plot. *Physica C: Superconductivity and Its Applications*, 548, 116–118.
- David, W.I.F., Harrison, W.T.A., Gunn, J.M.F., Moze, O., Soper, A.K., Day, P., Jorgensen, J.D., Hinks, D.G., Beno, M.A., Soderholm, L. and Capone II, D.W. (1987). Structure and crystal chemistry of the high-*T_c* superconductor YBa₂Cu₃O_{7-x}. *Nature*, 327(6120), 310–312.
- Deac, I. G., Burzo, E., Pop, A. V., Pop, V., Tetean, R., Kovacs, D., & Borodi, G. (1999). Intergranular properties of (Y_{1-xy}Zr_xCa_y) Ba₂Cu₃O_{7-δ} compounds. *International Journal of Modern Physics B*, 13(13), 1645–1654.
- Dew-Hughes, D. (1974). Flux pinning mechanisms in type II superconductors. *Philosophical Magazine*, 30(2), 293–305.

- Dew-Hughes, D. (2001). The critical current of superconductors: An historical review. *Low Temperature Physics*, 27(9–10), 713–722.
- Dihom, M.M., Shaari, A.H., Baqiah, H., Al-Hada, N.M., Chen, S.K., Azis, R.B.A.S., Kechik, M.M.A. & Abd-Shukor, R. (2017a). Effects of calcination temperature on microstructure and superconducting properties of Y123 ceramic prepared using thermal treatment method. *Solid State Phenomena*, 268, 325–329.
- Dihom, M. M., Shaari, A. H., Baqiah, H., Al-Hada, N. M., Kien, C. S., Azis, R. S., Kechik, M. M. A., Talib, Z. A., & Abd-Shukor, R. (2017b). Microstructure and superconducting properties of Ca substituted $Y(Ba_{1-x}Ca_x)_2Cu_3O_{7-\delta}$ ceramics prepared by thermal treatment method. *Results in Physics*, 7, 407–412.
- Dihom, M.M., Shaari, A.H., Baqiah, H., Al-Hada, N.M., Talib, Z.A., Kien, C.S., Azis, R.S., Kechik, M.M.A., Pah, L.K. and Abd-Shukor, R. (2017c). Structural and superconducting properties of $Y(Ba_{1-x}K_x)_2Cu_3O_{7-\delta}$ ceramics. *Ceramics International*, 43(14), 11339–11344.
- Dimos, D., Chaudhari, P., & Mannhart, J. (1990). Superconducting transport properties of grain boundaries in $YBa_2Cu_3O_7$ bicrystals. *Physical Review B*, 41(7), 4038–4049.
- Driscoll, D., Dombrowski, V., & Zhang, B. (2000). Development status of superconducting motors. *IEEE Power Engineering Review*, 20(5), 12–15.
- Duarte, E. A., Quintero, P. A., Meisel, M. W., & Nino, J. C. (2013). Electrospinning synthesis of superconducting BSCCO nanowires. *Physica C: Superconductivity and Its Applications*, 495, 109–113.
- Durný, R., Hautala, J., Ducharme, S., Lee, B., Symko, O. G., Taylor, P. C., Zheng, D. J., & Xu, J. A. (1987). Microwave absorption in the superconducting and normal phases of Y-Ba-Cu-O. *Physical Review B*, 36(4), 2361–2363.
- Dzul-Kifli, N. A. C., Kechik, M. M. A., Azam, S. H. M. N., Baqiah, H., Shaari, A. H., Lim, K. P., Chen, S. K., Yusuf, N. N. M., Sukor, S. I. A., & Miryala, M. (2021). Addition of KNO_3 on YBCO–123 in enhancing the structural and magnetic properties via thermal treatment method. *Solid State Science and Technology*, 29(1), 32–39.
- Dzul-Kifli, N. A. C., Kechik, M. M. A., Baqiah, H., Shaari, A. H., Lim, K. P., Chen, S. K., Sukor, S. I. A., Shabdin, M. K., Karim, M. K. A., Shariff, K. K. M., & Miryala, M. (2022). Superconducting Properties of $YBa_2Cu_3O_{7-\delta}$ with a Multiferroic Addition Synthesized by a Capping Agent-Aided Thermal Treatment Method. *Nanomaterials*, 12(22), 3958.
- Fatmasari, M., Alhad, H. A., Malitan, M. S. A., Salem, S. S. O., & Abd-Shukor, R. (2012). Superconducting and normal-state properties of $(Y_{1-x}Bi_x)Ba_2Cu_3O_{7-\delta}$ ($x = 0.00-0.30$). *Journal of Superconductivity and Novel Magnetism*, 25(2), 249–253.

- Foltyn, S. R., Civale, L., MacManus-Driscoll, J. L., Jia, Q. X., Maiorov, B., Wang, H., & Maley, M. (2007). Materials science challenges for high-temperature superconducting wire. *Nature Materials*, 6(9), 631–642.
- Forrest, A. M. (1983). Meissner and Ochsenfeld revisited. *European Journal of Physics*, 4(2), 117.
- Francavilla, T. L., Hein, R. A., & Liebenberg, D. H. (Eds.). (2013). Magnetic susceptibility of superconductors and other spin systems. *Springer Science & Business Media*.
- Ghahramani, S., Shams, G., & Soltani, Z. (2021). Comparative Investigation of the Effect of Titanium Oxide Nanoparticles on Some Superconducting Parameters of $Y_3Ba_5Cu_8O_{18\pm\delta}$ and $Y_1Ba_2Cu_3O_{7-\delta}$ Composites. *Journal of Electronic Materials*, 50(8), 4727–4740.
- Gomory, F. (1997). Characterization of high-temperature superconductors by AC susceptibility measurements. *Superconductor Science and Technology*, 10(8), 523–542.
- Goodarz Naseri, M., Saion, E. B., Abbastabar Ahangar, H., Shaari, A. H., & Hashim, M. (2010). Simple synthesis and characterization of cobalt ferrite nanoparticles by a thermal treatment method. *Journal of Nanomaterials*.
- Graf, T., Triscone, G., Junod, A., & Muller, J. (1990). Characterization and superconductivity of $YBa_2Cu_4O_8$ and $Y_2Ba_4Cu_7O_{14+x}$ and their intergrowths. *Physica B: Condensed Matter*, 165, 1671–1672.
- Grigorov, K., Tsaneva, V., Spasov, A., Matz, W., Groetzschel, R., & Reuther, H. (2002). RBS and ion channelling study of YBCO/STO and YBCO/LSMO/STO structures. Oxygen content estimated by X-ray diffraction. *Vacuum*, 69(1–3), 315–319.
- Hamadneh, I., Halim, S. A., & Lee, C. K. (2006). Characterization of $Bi_{1.6}Pb_{0.4}Sr_2Ca_2Cu_3O_y$ ceramic superconductor prepared via coprecipitation method at different sintering time. *Journal of Materials Science*, 41(17), 5526–5530.
- Hannachi, E., Slimani, Y., ben Azzouz, F.B., & Ekicibil, A. H. M. E. T. (2018). Higher intra-granular and inter-granular performances of YBCO superconductor with TiO_2 nano-sized particles addition. *Ceramics International*, 44(15), 18836–18843.
- Hannachi, E., Slimani, Y., Ekicibil, A. H. M. E. T., Manikandan, A., & ben Azzouz, F. B. (2019). Excess conductivity and AC susceptibility studies of Y–123 superconductor added with TiO_2 nano-wires. *Materials Chemistry and Physics*, 235, 121721.
- Hannachi, E., Almessiere, M. A., Slimani, Y., Baykal, A., & Ben Azzouz, F. (2020). AC susceptibility investigation of YBCO superconductor added by carbon nanotubes. *Journal of Alloys and Compounds*, 812, 152150.

- Hannachi, E., Almessiere, M. A., Slimani, Y., Alshamrani, R. B., Yasin, G., & Ben Azzouz, F. (2021). Preparation and characterization of high- T_c $(YBa_2Cu_3O_{7-\delta})_{1-x}/(CNTs)_x$ superconductors with highly boosted superconducting performances. *Ceramics International*, 47(16), 23539–23548.
- Hannachi, E., Mahmoud, K. A., Sayyed, M. I., & Slimani, Y. (2022). Effect of sintering conditions on the radiation shielding characteristics of YBCO superconducting ceramics. *Journal of Physics and Chemistry of Solids*, 164, 110627.
- Hari Babu, N., Iida, K., & Cardwell, D. A. (2006). Enhanced magnetic flux pinning in nano-composite Y-Ba-Cu-O superconductors. *Physica C: Superconductivity and Its Applications*, 445–448(1–2), 353–356.
- Hassenzahl, W. V. (2001). Superconductivity, an enabling technology for 21st century power systems? *IEEE Transactions on Applied Superconductivity*, 11(1), 1447–1453.
- Hayashi, H., Tsutsumi, K., Saho, N., Nishizima, N., & Asano, K. (2003). Study on a mobile-type magnetic separator applying high- T_c bulk superconductors. *Physica C: Superconductivity and Its Applications*, 392–396, 745–748.
- Hirsch, J. E. (2007). Do superconductors violate Lenz's law? Body rotation under field cooling and theoretical implications. *Physics Letters A: General, Atomic and Solid State Physics*, 366(6), 615–619.
- Hirsch, J. E. (2009). BCS theory of superconductivity: It is time to question its validity. *Physica Scripta*, 80(3), 035702.
- Hirsch, J. E. (2012). The origin of the Meissner effect in new and old superconductors. *Physica Scripta*, 85(3), 035704.
- Hsiao, Y. J., Chang, Y. H., Chang, Y. S., Fang, T. H., Chai, Y. L., Chen, G. J., & Huang, T. W. (2007). Growth and characterization of $NaNbO_3$ synthesized using reaction-sintering method. *Materials Science and Engineering B: Solid-State Materials for Advanced Technology*, 136(2–3), 129–133.
- Huang, T.W., Wu, N.C., Chou, Y.H., Lin, W.T., Wu, T.C., Chin, T.S., Wu, P.T., Yen, H.H. and Chen, Y.C., (1988). The formation of superconducting $YBa_2Cu_3O_{7-x}$ through solid state reaction. *Journal of crystal growth*, 91(3), 402–409.
- Hull, J. R. (1997). Flywheels on a roll. *IEEE Spectrum*, 34(7), 20–25.
- Hull, J. R. (2000). Superconducting bearings. *Superconductor Science and Technology*, 13(2), R1.
- Inoue, K., Miyake, Y., Miryala, M., & Murakami, M. (2017). Effects of carbon nanotube addition on superconductivity in Y-Ba-Cu-O bulk superconductors. *Journal of Physics: Conference Series* 871, (1), 012051.

- Izumi, F., Asano, H., Ishigaki, T., Takayama-Muromachi, E., Uchida, Y., & Watanabe, N. (1987). Crystal structure of the orthorhombic form of $\text{Ba}_2\text{YCu}_3\text{O}_{7-x}$ at 42 k. *Japanese Journal of Applied Physics*, 26(7A), 1193–1196.
- Jannah, A. N., Ilhamsyah, A. B. P., & Abd-Shukor, R. (2021). AC susceptibility and electrical properties of Ta substituted ($\text{Ta}_{1-x}\text{Ta}_x$) (BaSr) CaCu_2O_7 superconductor ($x = 0-0.3$). *Cryogenics*, 113, 103222.
- Jensen, R.P. (2016). *Structural investigation of $\text{La}_{2-x}\text{Sr}_x\text{CuO}_{4+y}$ following staging as a function of temperature*, MSc. thesis, University of Copenhagen, Denmark.
- Jorgensen, J. D., Beno, M. A., Hinks, D. G., Soderholm, L., Volin, K. J., Segre, C. U., Zhang, K., & Kleefisch, M. S. (1987). Oxygen ordering and the orthorhombic-to-tetragonal phase transition in $\text{Ba}_2\text{YCu}_3\text{O}_{7-x}$. *Physical Review B*, 36(7), 3608–3616.
- Josephson, B. D. (1962). Possible new effects in superconductive tunnelling. *Physics Letters*, 1(7), 251–253.
- Kamarudin, A. N., Kechik, M. M. A., Abdullah, S. N., Baqiah, H., Chen, S. K., Karim, M. K. A., Ramli, A., Lim, K. P., Shaari, A. H., Miryala, M., Murakami, M., & Talib, Z. A. (2022). Effect of Graphene Nanoparticles Addition on Superconductivity of $\text{YBa}_2\text{Cu}_3\text{O}_{7-\delta}$ Synthesized via the Thermal Treatment Method. *Coatings*, 12(1), 1–13.
- Kasap, S., Koughia, C., & Ruda, H. E. (2017). Electrical Conduction in Metals and Semiconductors. *Springer Handbook of Electronic and Photonic Materials*, 1–1.
- Kelley, N., Nassi, M., & Masur, L. (2001). Application of HTS wire and cables to power transmission: State of the art and opportunities. *IEEE Power Engineering Society Winter Meeting. Conference Proceedings*, 2, 448–454.
- Khalid, N. A., Kechik, M. M. A., Baharuddin, N. A., Kien, C. S., Baqiah, H., Yusuf, N. N. M., Shaari, A. H., Hashim, A., & Talib, Z. A. (2018). Impact of carbon nanotubes addition on transport and superconducting properties of $\text{YBa}_2\text{Cu}_3\text{O}_{7-\delta}$ ceramics. *Ceramics International*, 44(8), 9568–9573.
- Khan, H., Yerramilli, A. S., D'Oliveira, A., Alford, T. L., Boffito, D. C., & Patience, G. S. (2020). Experimental methods in chemical engineering: X-ray diffraction spectroscopy–XRD. *Canadian Journal of Chemical Engineering*, 98(6), 1255–1266.
- Kittel, C. (2005). *Introduction to solid state physics*, 8th ed. Wiley New York.
- Kleiner, R., & Buckel, W. (2016). *Superconductivity: an introduction*. Weinheim: Wiley-VCH.
- Kovalev, L. K., Ilushin, K. v., Koneev, S. M. A., Kovalev, K. L., Penkin, V. T., Poltavets, V. N., Gawalek, W., Habisreuther, T., Oswald, B., & Best, K. J. (1999). Hysteresis and reluctance electric machines with bulk HTS rotor elements. *IEEE Transactions on Applied Superconductivity*, 9(2), 1261–1264.

- Kuang, M. Q., Wu, S. Y., Yuan, H. K., Wang, L. D., Duan, S. K., Kuang, A. L., & Li, G. Q. (2017). Pseudogap of Ortho-III $\text{YBa}_2\text{Cu}_3\text{O}_{7-x}$ from Cu EPR investigation. *Journal of Alloys and Compounds*, 690, 169–175.
- Larbalestier, D. (1996). Superconductor Flux Pinning and Grain Boundary Control. *Science*, 274(5288), 736–737.
- Lee, C. Y., & Kao, Y. H. (1995). Low-field magnetic susceptibility studies of high- T_c superconductors. *Physica C: Superconductivity*, 241(1–2), 167–180.
- Lee, P. J., Saion, E., Al-Hada, N. M., & Soltani, N. (2015). A simple up-scalable thermal treatment method for synthesis of ZnO nanoparticles. *Metals*, 5(4), 2383–2392.
- Lian, Z., Pingxiang, Z., Ping, J., Keguang, W., Jingrong, W., & Xiaozu, W. (1990). The properties of YBCO superconductors prepared by a new approach: The “powder melting process.” *Superconductor Science and Technology*, 3(10), 490–492.
- London, F., & London, H. (1935). The Electromagnetic Equations of the Supraconductor. Proceedings of the Royal Society of London. *Series A-Mathematical and Physical Sciences*, 149(866), 71–88.
- Maaz, K., Karim, S., Mumtaz, A., Hasanain, S. K., Liu, J., & Duan, J. L. (2009). Synthesis and magnetic characterization of nickel ferrite nanoparticles prepared by co-precipitation route. *Journal of Magnetism and Magnetic Materials*, 321(12), 1838–1842.
- Maeda, H., Tanaka, Y., Fukutomi, M., & Asano, T. (1988). A new High- T_c oxide superconductor without a rare earth element. *Japanese Journal of Applied Physics*, 27(2A), L209–L210.
- Manthiram, A., & Goodenough, J. B. (1987). Synthesis of the high- T_c superconductor $\text{YBa}_2\text{Cu}_3\text{O}_{7-\delta}$ in small particle size. *Nature*, 329, 701–703.
- Manthiram, A., Lee, S. J., & Goodenough, J. B. (1988). Influence of Ca on the superconductivity of $\text{Y}_{1-x}\text{Ca}_x\text{Ba}_2\text{Cu}_3\text{O}_{7-\delta}$. *Journal of Solid State Chemistry*, 73(1), 278–282.
- Matsushita, T. (2007). *Flux pinning in superconductors*. (Vol. 164). Berlin: Springer.
- Mellekh, A., Zouaoui, M., ben Azzouz, F., Annabi, M., & ben Salem, M. (2006). Nano- Al_2O_3 particle addition effects on $\text{YBa}_2\text{Cu}_3\text{O}_y$ superconducting properties. *Solid State Communications*, 140(6), 318–323.
- Melnikov, P., Nascimento, V. A., Consolo, L. Z. Z., & Silva, A. F. (2013). Mechanism of thermal decomposition of yttrium nitrate hexahydrate, $\text{Y}(\text{NO}_3)_3 \cdot 6\text{H}_2\text{O}$ and modeling of intermediate oxynitrates. *Journal of Thermal Analysis and Calorimetry*, 111(1), 115–119.
- Menzel, Joseph D. II. Prime, R. B. (Eds.). (2009). *Thermal Analysis of Polymers Fundamentals and Applications*. Hoboken: John Wiley & Sons.

- Misra, S. K., & Misiak, L. E. (1989). An EPR investigation of the high- T_c superconductor $\text{YBa}_{1.9}\text{Na}_{0.1}\text{Cu}_3\text{O}_{7-\delta}$. *Condens. Matter*, 1(47), 9499.
- Mohanta, A., & Behera, D. (2011). Effect of granularity and inhomogeneity in excess conductivity of $\text{YBa}_2\text{Cu}_3\text{O}_{7-\delta+x}\text{BaTiO}_3$ superconductor. *Physica B: Condensed Matter*, 406(4), 877–884.
- Mohd Yusuf, Nur Nabilah. (2018a). *Influence of NbO_2 and SnO_2 Additions on the Properties of $\text{YBa}_2\text{Cu}_3\text{O}_{7-d}$ Bulk Superconductor Synthesised Via Thermal Treatment Method*, MSc. Thesis, Universiti Putra Malaysia.
- Mohd Yusuf, N.N., Awang Kechik, M.M., Baqiah, H., Soo Kien, C., Kean Pah, L., Shaari, A.H., Wan Jusoh, W.N.W., Abd Sukor, S.I., Mousa Dihom, M., Talib, Z.A. and Abd-Shukor, R. (2018b). Structural and superconducting properties of thermal treatment-synthesised bulk $\text{YBa}_2\text{Cu}_3\text{O}_{7-\delta}$ superconductor: Effect of addition of SnO_2 nanoparticles. *Materials*, 12(1), 92.
- Mourachkine, A. (2004). *Room-temperature superconductivity*. Cambridge Int Science Publishing.
- Mousumibala Sahoo. (2015). *Study of structure and electrical transport property in composite and doped system of $\text{YBa}_2\text{Cu}_3\text{O}_{7-x}$ superconductor*, PhD Thesis. National Institute of Technology, India.
- Muhammad-Najib, K., & Abd-Shukor, R. (2020). Microstructure, AC susceptibility and electrical properties of K_2CO_3 added $\text{YBa}_2\text{Cu}_3\text{O}_{7-\delta}$ superconductor. *Cryogenics*, 109, 103099.
- Müller, K. H. (1989). AC susceptibility of high temperature superconductors in a critical state model. *Physica C: Superconductivity and Its Applications*, 159(6), 717–726.
- Nagamatsu, J., Nakagawa, N., Muranaka, T., Zenitani, Y., & Akimitsu, J. (2001). Superconductivity at 39 K in magnesium diboride. *Nature*, 410(6824), 63–64.
- Naseri, M. G., Saion, E. B., Ahangar, H. A., Hashim, M., & Shaari, A. H. (2011). Simple preparation and characterization of nickel ferrite nanocrystals by a thermal treatment method. *Powder Technology*, 212(1), 80–88.
- Nikolo, M. (1995). Superconductivity: A guide to alternating current susceptibility measurements and alternating current susceptometer design. *American Journal of Physics*, 63(1), 57–65.
- Nur-Akasyah, J., Nur-Shamimie, N. H., & Abd-Shukor, R. (2017). Effect of CdTe Addition on the Electrical Properties and AC Susceptibility of $\text{YBa}_2\text{Cu}_3\text{O}_{7-\delta}$ Superconductor. *Journal of Superconductivity and Novel Magnetism*, 30(12), 3361–3365.
- Nur-Syazwani, A. C. A., & Abd-Shukor, R. (2019). Effect of Ferrimagnetic Cr_2S_3 on AC Susceptibility and Superconducting Properties of $\text{YBa}_2\text{Cu}_3\text{O}_{7-\delta}$. *Journal of Superconductivity and Novel Magnetism*, 32, 863–868.

- Ochsenkühn-Petropoulou, M., Argyropoulou, R., Tarantilis, P., Kokkinos, E., Ochsenkühn, K. M., & Parissakis, G. (2002). Comparison of the oxalate coprecipitation and the solid state reaction methods for the production of high temperature superconducting powders and coatings. *Journal of Materials Processing Technology*, 127(1), 122–128.
- Oswald, B., Krone, M., Söll, M., Straßer, T., Oswald, J., Best, K. J., Gawalek, W., & Kovalev, L. (1999). Superconducting reluctance motors with YBCO bulk material. *IEEE Transactions on Applied Superconductivity*, 9(2), 1201–1204.
- Panagopoulos, C., & Xiang, T. (1998). Relationship between the superconducting energy gap and the critical temperature in high- T_c superconductors. *Physical Review Letters*, 81(11), 2336–2339.
- Patternson, A. L. (1939). Scherrer Formula for X-ray Particle Size Determination. *Physical Review*, 56(10), 978.
- Pechoniy, A. P., Glinchuk, M. D., Miheev, V. A., & Babich, I. G. (1990). ESR and magnetic susceptibility of localized Cu magnetic moments in YBCO-ceramics. *Phase Transitions: A Multinational Journal*, 29(2), 105–114.
- Pęczkowski, P., Zachariasz, P., Kowalik, M., Zalecki, R., & Jastrzębski, C. (2019). Characterization of the superconductor-multiferroic type materials based on $\text{YBa}_2\text{Cu}_3\text{O}_{7-\delta}$ - YMnO_3 composites. *Ceramics International*, 45(15), 18189–18204.
- Presland, M. R., Tallon, J. L., Buckley, R. G., Liu, R. S., & Flower, N. E. (1991). General trends in oxygen stoichiometry effects on T_c in Bi and Tl superconductors. *Physica C: Superconductivity and Its Applications*, 176(1–3), 95–105.
- Quanli, J., Haijun, Z., Suping, L., & Xiaolin, J. (2007). Effect of particle size on oxidation of silicon carbide powders. *Ceramics International*, 33(2), 309–313.
- Rabinowitz, M. (2000). Superconducting power generation. *IEEE Power Engineering Review*, 20(5), 8–11.
- Ramli, A., Shaari, A. H., Baqiah, H., Kean, C. S., Kechik, M. M. A., & Talib, Z. A. (2016). Role of Nd_2O_3 nanoparticles addition on microstructural and superconducting properties of $\text{YBa}_2\text{Cu}_3\text{O}_{7-\delta}$ ceramics. *Journal of Rare Earths*, 34(9), 895–900.
- Rani, P., Jha, R., & Awana, V. P. S. (2013). AC susceptibility study of superconducting $\text{YBa}_2\text{Cu}_3\text{O}_7$: Ag_x bulk composites ($x = 0.0$ - 0.20): The role of intra and intergranular coupling. *Journal of Superconductivity and Novel Magnetism*, 26(7), 2347–2352.
- Regnier, S., Alfred-Duplan, C., Vacquier, G., & Marfaing, J. (1996). Effect of Mn inclusion in superconducting YBCO-based composites. *Applied Superconductivity*, 4(1–2), 41–51.

- Rejith, P. P., Vidya, S., & Thomas, J. K. (2015). Improvement of Critical Current Density in $\text{YBa}_2\text{Cu}_3\text{O}_{7-\delta}$ Superconductor with Nano TiO_2 Addition. *Materials Today: Proceedings*, 2(3), 997–1001.
- Rodriguez, J., & Lazo, A. (2018). Synthesis of YBCO superconductor by the method of combustion reaction in solution. *Journal of Physics: Conference Series*, 1143(1), 012029. IOP Publishing.
- Rotta, M., Motta, M., Pessoa, A. L., Carvalho, C. L., Deimling, C. V., Lisboa-Filho, P. N., Ortiz, W. A., & Zadorosny, R. (2020). One-pot-like facile synthesis of $\text{YBa}_2\text{Cu}_3\text{O}_{7-\delta}$ superconducting ceramic: Using PVP to obtain a precursor solution in two steps. *Materials Chemistry and Physics*, 243, 122607.
- Sahoo, B., Mohapatra, S. R., Singh, A. K., Samal, D., & Behera, D. (2019a). Effects of CNTs blending on the superconducting parameters of YBCO superconductor. *Ceramics International*, 45(6), 7709–7716.
- Sahoo, B., Routray, K. L., Mirdha, G. C., Karmakar, S., Singh, A. K., Samal, D., & Behera, D. (2019b). Investigation of microhardness and superconducting parameters of CNTs blended YBCO superconductor. *Ceramics International*, 45(17), 22055–22066.
- Sahoo, B., Routray, K. L., Samal, D., & Behera, D. (2019c). Effect of artificial pinning centers on YBCO high temperature superconductor through substitution of graphene nano-platelets. *Materials Chemistry and Physics*, 223, 784–788.
- Sauv, K., Nicolas, M., Van Huong, C. N., Dubon, A., Legeay, P., & Kandel, L. (1993). Effect of a barium deficiency on the structural and magnetic properties of $\text{RE Ba}_{2-x}\text{Cu}_3\text{O}_z$ (RE=Y, Nd, Eu, Er, Yb). *Superconductor Science and Technology*, 6(5), 327–336.
- Saxena, A. K. (2012). *High-Temperature Superconductors*. (Vol. 125). New York: Springer Science & Business Media.
- Shaaidi, W. N. A. W., Lim, K. P., Matori, K. A., Saion, E., Halim, S. A., & Chen, S. K. (2014). The superconductivity of $\text{YBa}_2\text{Cu}_3\text{O}_{7-d}$ reacted with nano-SiC. *Solid State Science and Technology*, 22(1 & 2), 132–138.
- Sharma, R. G. (2021). *Superconductivity: Basics and Applications to Magnets*. (Vol. 214). New York: Springer Nature.
- Sheahen, T. P. (2002). *Introduction to High-Temperature Superconductivity*. Springer Science & Business Media.
- Shekhar, C., Giri, R., Malik, S. K., & Srivastava, O. N. (2007). Improved critical current density of MgB_2 -carbon nanotubes composite. *Journal of Nanoscience and Nanotechnology*, 7(6), 1804–1809.
- Shen, Z., Wang, Y., Chen, W., Fei, L., Li, K., Chan, H. L. W., & Bing, L. (2013). Electrospinning preparation and high-temperature superconductivity of $\text{YBa}_2\text{Cu}_3\text{O}_{7-x}$ nanotubes. *Journal of Materials Science*, 48(11), 3985–3990.

- Sheng, Z. Z., Sheng, L., Su, H. M., & Hermann, A. M. (1988). Tl_2O_3 vapor process of making Tl-Ba-Ca-Cu-O superconductors. *Applied Physics Letters*, *53*, 2686–2688.
- Slimani, Y., Hannachi, E., Salem, M. B., Hamrita, A., Varilci, A., Dachraoui, W., Salem M. B., & Azzouz, F. B. (2014). Comparative study of nano-sized particles $CoFe_2O_4$ effects on superconducting properties of Y-123 and Y-358. *Physica B: Condensed Matter*, *450*, 7-15.
- Slimani, Y., Hannachi, E., Hamrita, A., Ben Salem, M. K., Ben Azzouz, F.B., Manikandan, A., & Ben Salem, M. (2018). Comparative investigation of the ball milling role against hand grinding on microstructure, transport and pinning properties of $Y_3Ba_5Cu_8O_{18\pm\delta}$ and $YBa_2Cu_3O_{7-\delta}$. *Ceramics International*, *44*(16), 19950–19957.
- Slimani, Y., Hannachi, E., Ekicibil, A. H. M. E. T., Almessiere, M. A., & ben Azzouz, F. B. (2019a). Investigation of the impact of nano-sized wires and particles TiO_2 on Y-123 superconductor performance. *Journal of Alloys and Compounds*, *781*, 664–673.
- Slimani, Y., Almessiere, M. A., Hannachi, E., Al-qwairi, F. O., Manikandan, A., Baykal, A., & Ben Azzouz, F. B. (2019b). AC susceptibility, DC magnetization and superconducting properties of tungsten oxide nanowires added $YBa_2Cu_3O_y$. *Ceramics International*, *45*(17), 21864–21869.
- Slimani, Y., Almessiere, M. A., Hannachi, E., Mumtaz, M., Manikandan, A., Baykal, A., & Ben Azzouz, F. B. (2019c). Improvement of flux pinning ability by tungsten oxide nanoparticles added in $YBa_2Cu_3O_y$ superconductor. *Ceramics International*, *45*(6), 6828–6835.
- Strauven, H., Locquet, J. P., Verbeke, O. B., & Bruynseraede, Y. (1988). Oxygen evolution from $YBa_2Cu_3O_{6.85}$ high T_c superconductors. *Solid State Communications*, *65*(4), 293–296.
- Tachiki, M., & Takahashi, S. (1989). Anisotropy of critical current in layered oxide superconductors. *Solid State Communications*, *72*(11), 1083–1086.
- Takahashi, H., Igawa, K., Arii, K., Kamihara, Y., Hirano, M., & Hosono, H. (2008). Superconductivity at 43 K in an iron-based layered compound $LaO_{1-x}F_xFeAs$. *Nature*, *453*(7193), 376–378.
- Tallon, J. L., Bernhard, C., Shaked, H., Hitterman, R. L., & Jorgensen, J. D. (1995). Generic superconducting phase behavior in high- T_c cuprates: T_c variation with hole concentration in $YBa_2Cu_3O_{7-\delta}$. *Physical Review B*, *51*(18), 911–914.
- Tanaka, S. (1987). Possibility of two-dimensional superconductivity in $(La, Ba)_2CuO_4$ and $(La, Sr)_2CuO_4$ with high critical temperatures. *Japanese Journal of Applied Physics*, *26*(3 A), L203–L205.

- Tanaka, S. (2006). High-temperature superconductivity. *Japanese Journal of Applied Physics*, 45(12), 9011–9024.
- Timusk, T., & Statt, B. (1999). The pseudogap in high-temperature superconductors: an experimental survey. *Reports on Progress in Physics*, 62(1), 61–122.
- Tomita, M., & Murakami, M. (2003). High-temperature superconductor bulk magnets that can trap magnetic fields of over 17 teslas at 29 K. *Nature*, 421(6922), 517–520.
- Tranquada, J. M., Heald, S. M., Moodenbaugh, A. R., & Xu, Y. (1988). Mixed valency, hole concentration, and T_c in $\text{YBa}_2\text{Cu}_3\text{O}_{6+x}$. *Physical Review B*, 38(13), 8893–8899.
- Ungár, T. J. S. M. (2004). Microstructural parameters from X-ray diffraction peak broadening. *Scripta Materialia*, 51(8), 777–781.
- Uysal, E., Ozturk, A., Kutuk, S. E. Z. A. İ., & Çelebi, S. (2014). Effects of Lu Doping on the Magnetic Behavior of YBCO Superconductors Prepared by MPMG Method. *Journal of Superconductivity and Novel Magnetism*, 27(9), 1997–2003.
- Vanderbemden, P., Cloots, R., Ausloos, M., Doyle, R.A., Bradley, A.D., Lo, W., Cardwell, D.A. and Campbell, A.M. (1999). Intragranular and intergranular superconducting properties of bulk melt-textured YBCO. *IEEE Transactions on Applied Superconductivity*, 9(2), 2308–2311.
- Wang, J., Gamchi, H. S., Taylor, K. N. R., Russell, G. J., & Yue, Y. (1993). Field dependent AC loss in YBCO superconductors. *Physica C: Superconductivity and Its Applications*, 205(3–4), 363–370.
- Wei, K., Ing, K., Hamdan, M. S., Radiman, S., & Abd-Shukor, R. (2018). AC Susceptibility and Superconducting Properties of Graphene Added $\text{YBa}_2\text{Cu}_3\text{O}_{7-d}$. *Journal of Superconductivity and Novel Magnetism*, 31(9), 2699–2703.
- Wei, X., Nagarajan, R. S., Peng, E., Xue, J., Wang, J., & Ding, J. (2016). Fabrication of $\text{YBa}_2\text{Cu}_3\text{O}_{7-x}$ (YBCO) superconductor bulk structures by extrusion free forming. *Ceramics International*, 42(14), 15836–15842.
- Wu, M. K., Ashburn, J. R., Torng, C. J., Hor, P. H., Meng, R. L., Gao, L., Huang, Z. J., Wang, Y. Q., & Chu, C. W. (1987). Superconductivity at 93 K in a new mixed-phase Yb-Ba-Cu-O compound system at ambient pressure. *Physical Review Letters*, 58(9), 908–910.
- Xiong, Y., Washio, I., Chen, J., Cai, H., Li, Z. Y., & Xia, Y. (2006). Poly (vinyl pyrrolidone): a dual functional reductant and stabilizer for the facile synthesis of noble metal nanoplates in aqueous solutions. *Langmuir*, 22(20), 8563–8570.
- Xu, H. H., Cheng, L., Yan, S. B., Yu, D. J., Guo, L. S., & Yao, X. (2012). Recycling failed bulk YBCO superconductors using the NdBCO/YBCO/MgO film-seeded top-seeded melt growth method. *Journal of Applied Physics*, 111(10), 103910.

- Xu, X. L., Guo, J. D., Wang, Y. Z., & Sozzi, A. (2002). Synthesis of nanoscale superconducting YBCO by a novel technique. *Physica C: Superconductivity and Its Applications*, 371(2), 129–132.
- Yang, C. M., Chen, P. W., Liu, C. J., Chen, S. Y., Kuo, C. S., Chen, I. G., & Wu, M. K. (2017). Effect of ZnO/TiO₂ Nanorods Fabricated Using the Electrospinning Method in Y-Ba-Cu-O Single Grain Bulk Superconductors. *IEEE Transactions on Applied Superconductivity*, 27(4), 4–7.
- Yang, M., Kao, Y. H., Xin, Y., & Wong, K. W. (1994). Chemical doping and intergranular magnetic-field effects in bulk thallium-based superconductors. *Physical Review B*, 50(18), 13653.
- Yang, W. M., & Wang, M. (2013). New method for introducing nanometer flux pinning centers into single domain YBCO bulk superconductors. *Physica C: Superconductivity and Its Applications*, 493, 128–131.
- Yang, Y. M., Out, P., Zhao, B. R., Zhao, Y. Y., Li, L., Ran, Q. Z., & Jin, R. Y. (1989). Characterization of YBa₂Cu₃O_{7-x} bulk samples prepared by citrate synthesis and solid-state reaction. *Journal of Applied Physics*, 66(1), 312–315.
- Yang, Z. Q., Su, X. D., Zhang, C., Qiao, G. W., & Han, W. (1998). The influence of nano-SiC on the flux pinning of YBa₂Cu₃O_{7-y}/nano-SiC composites. *Physica Status Solidi (A)*, 167(1), 165–173.
- Yanmaz, E. K. R. E. M., Balci, S. Ü. L. E. Y. M. A. N., & Küçükömeroğlu, T. (2001). Magnetic properties of melt textured YBa₂Cu₃O_{7-d} with TiO₂ dopant. *Materials Letters*, 54(2–3), 191–199.
- Yap, S.H., Kechik, M.M., Chen, S.K., Kamarudin, A.N., Baqiah, H., Lim, K.P., Karim, M.K.A., Halim, S.A., Doyan, A. and Shariff, K.K. (2023). Comparative Study on Superconducting Properties and surface morphology analysis for Y_{0.85}K_{0.15}Ba₂Cu₃O_{7-δ} and Y_{0.85}Ca_{0.15}Ba₂Cu₃O_{7-δ} synthesized via thermal treatment method. In *AIP Conference Proceedings*, 2619(1). AIP Publishing.
- Yuh, J., Perez, L., Sigmund, W. M., & Nino, J. C. (2007). Sol-gel based synthesis of complex oxide nanofibers. *Journal of Sol-Gel Science and Technology*, 42(3), 323–329.